 Bull. Chem. Soc. Jpn. Vol. 80, No. 7, 1307–1315 (2007)

Dual Fluorescence in a Schiff Base Derived from an Acridinedione Dye. Excited State Intramolecular Proton Transfer

Viruthachalam Thiagarajan[†] **and Perumal Ramamurthy***

National Centre for Ultrafast Processes, University of Madras, Taramani Campus, Chennai-600 113, India

Department of Inorganic Chemistry, University of Madras, Guindy Campus, Chennai-600 025, India

Received October 11, 2006; E-mail: prm60@hotmail.com

Newly synthesized nonconjugated, but covalently linked, bichromophoric systems (ADDSA) contain a salicylideneaniline (SA) moiety linked to an acridinedione (ADD) fluorophore via a covalent bond. The absorption and fluorescence characteristics of the ADDSA systems in various solvents reveal that the dual fluorescence originates from two different chromophores in the same molecule. The solvent polarity independent, long wavelength anomalous emission originates from the keto form of SA moiety via excited state intramolecular proton transfer (ESIPT). The ESIPT pathway was further confirmed by the benzylideneaniline (BA) and ADD moieties coupled non-proton transfer model system (ADDBA). Absence of the longer wavelength anomalous emission in the steady state as well as the shorter lifetime component in the time-resolved study for ADDBA system supports ESIPT mechanism for long wavelength anomalous emission in ADDSA system.

ESIPT, discovered by Weller in 1955, has been the subject of continuous interest of researchers for more than five decades.[1] Photoinduced proton transfer, which is a representative of a limited number of adiabatic photochemical processes giving rise to fluorescence with an abnormally large Stokes shift,[2] plays an important role in biophysics,[3] and has practical application in technology, for example, in organic scintillators.[4] Among the molecular systems characterised by excited state proton transfer, both efficient organic photochromes[5] and polymer ultraviolet stabilisers[6] are of much interest. Prospects for the use of ESIPT systems in luminescent solar energy concentrators have also been discussed in literature.[7] For the ESIPT reaction to occur, it is necessary that proton-donor and proton-acceptor moieties be in close proximity and conjugated to one another in an organic molecule. ESIPT is considered as the driving force for the concerted enhancement of their acidity or basicity upon the transition to an excited state.[8] If a molecule carries its own base, excited-state proton transfer can occur intramolecularly and becomes more or less independent of the surrounding solvent. ESIPT reaction is extremely fast (subpicosecond kinetics) and also occurs in rigid glasses and at very low temperatures.[9] Very often, only the ESIPT product (P*) fluoresces, and this is the source of extremely large Stokes shift, which are fairly independent of medium and temperature. Thus, ESIPT dyes are ideal candidates for use as fluorescence labels in order to avoid interference from other fluorescent material present in the sample to be analyzed.

Most of the publications on ESIPT deal with derivatives of salicylic acid, its esters and amides,[10] salicylaldehyde, acetophenone and related compounds,[11] *o*-hydroxybenzoxazoles,[12] benzothiazoles,[13] triazoles,[14] flavonols,[15] anthraquinones,[16] bipyridyls,[17] and malonic aldehyde.[18] Recently, Chou et al. have studied the solvent polarity tuned excited state, charge-transfer-coupled proton transfer reaction in *p*-*N*,*N*-ditolylaminosalicylaldehyde- and 3-hydroxyflavone-based systems.[19]

Orthohydroxy Schiff bases appear to be interesting compounds due to their thermochromic and photochromic properties related to intramolecular proton-transfer reactions. It makes them potential materials for optical memory and optical switches.[20] Considerable interest has been focused on salicylideneaniline (SA), which is the simplest of the anil compounds. On the basis of X-ray crystallography, and electronic and vibrational spectroscopy, SA in the crystalline state is predominantly in the enol form.[21] It is generally accepted that in such photoexcited, internally hydrogen-bonded systems, the proton is quickly translocated from the oxygen towards the nitrogen atom and a keto-like species is formed in the singlet excited state. Studies of salicylideneanilines have been extended to molecules possessing two identical proton-transfer centres (BSP, BSD) by Grabowska et al.[22] Substituent effects on the ground state properties of naphthalene analogues of salicylideneaniline have been studied by Ohshima et al.[23]

Acridinedione (ADD) dyes have been developed recently, as a family of efficient laser dyes[24] and these dyes are structurally similar to NADH.[25] ADD is a bifunctional molecule, and due to this nature, it acts both as an electron donor and acceptor. It has been observed that the spectral properties and the photophysics of the ADD dyes are largely influenced by the nature of the substituents at the para position of the phenyl group.[26,27] ADD dyes have also been used as photoinitiators for polymerization of acrylates and methyl acrylates.[28] These dyes have also been used as a photosensitizer for the onium salt decomposition.[29]

We are particularly interested in the photophysical properties of nonconjugated but covalently linked, bichromophoric

† Present address: Department of Chemistry, Graduate School of Science, Tohoku University, Sendai 980-8578

Published on the web July 11, 2007; doi:10.1246/bcsj.80.1307

systems, which show dual fluorescence due to the occurrence of one or two of the following three mechanisms: photoinduced electron transfer (PET), photoinduced charge transfer (PCT), and ESIPT.[26] Transition-metal ion or anion recognition induces a change in the photophysical properties of the fluorophore due to change in the oxidation potential of the donor group, which results in fluorescence enhancement or quenching.[26,30] This study will help to understand the photophysical properties of dual emitting ADD dyes and their interaction with ions.

One of the most important issues of current interest is ESIPT reactions associated with intramolecular charge transfer (ICT) within the same molecule. Newly synthesized bichromophoric ADDSA systems contain salicylideneaniline (SA) moiety connected to the ADD fluorophore via covalent bond. ADDSA systems show dual fluorescence in aprotic solvents, and in order to elucidate the exact mechanism for the dual fluorescence, the following ADD dyes were selected (Scheme 1).

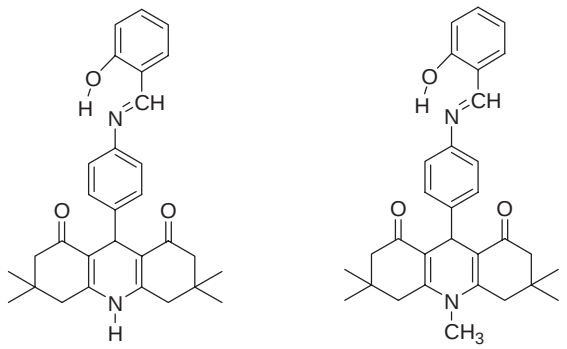

Scheme 1.

Results and Discussion

Steady State Spectral Studies. The absorption spectral studies of ADDSA-1 in a series of protic and aprotic solvents have been carried out. Table 1 summarizes the absorption characteristics of ADDSA-1 in different solvents. The absorption spectra of ADDSA-1 in both protic and aprotic solvents were similar, and they showed a strong absorption band at 350 nm. The absorption spectrum of ADDSA-1 in methanol and acetonitrile are presented in Fig. 1.

The emission spectra were recorded in various solvents after exciting the dye at its longer wavelength absorption maximum (350 nm). The emission spectrum of ADDSA-1 recorded in different solvents is shown in Fig. 2. The emission spectrum of ADDSA-1 showed a single peak in protic solvents whereas in aprotic solvents it shows two distinct peaks: a shorter wavelength local excited fluorescence around 425 nm and a new anomalous longer wavelength emission around 528 nm. Table 1 lists the emission characteristics of ADDSA-1 in various solvents. The shorter wavelength emission around 425 nm was assigned to the CT from the ring nitrogen to ring carbonyl oxygen center within the ADD fluorophore (local excited, LE), which was found to shift towards lower energies with increasing solvent polarity and this shift is due to the stabilization of the CT state.[31] In contrast to the lower wavelength emission, the anomalous longer wavelength emission maximum was independent of solvent polarity, and it was more intensed in aprotic nonpolar solvents. The concentration independent nature of the ratio of 425 and 528 nm emission intensity shoes that an excimer or exciplex did not form.

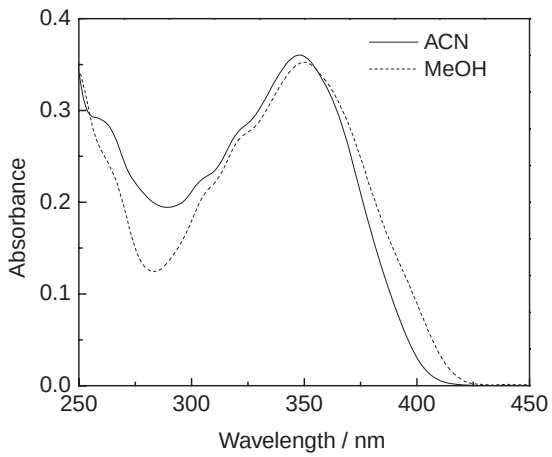

Fig. 1. Absorption spectrum of ADDSA-1 in acetonitrile and methanol.

Table 1. Absorption and Fluorescence Spectral Data of ADDSA-1, ADDSA-2, and ADDBA in Various Solvents

	Absorption, λ_{max}/nm			Fluorescence, λ_{max}/nm[a)]		
Solvent	ADDSA-1	ADDSA-2	ADDBA	ADDSA-1	ADDSA-2	ADDBA
Toluene	350	350	340	404, 531	430, 530(s)	426
Dichloromethane	349	351	340	419, 527	438, 530(s)	432
Acetone	348	348	328	416, 527	440, 530(s)	434
Acetonitrile	348	349	334	425, 528	441, 530(s)	439
DMSO	350	350	337	430, 527	440, 530(s)	438
Methanol	348	348	325	435	452	451

a) (s), shoulder.

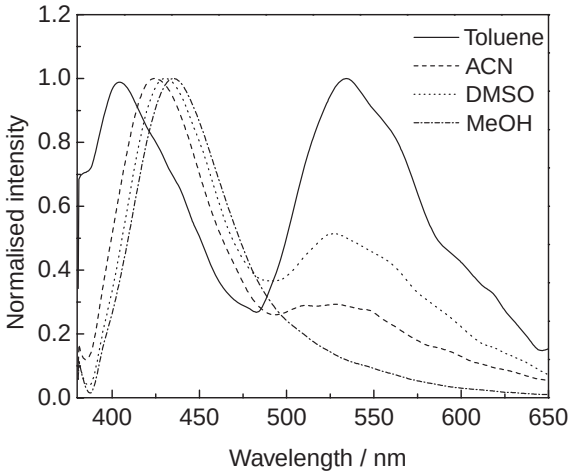

Fig. 2. Emission spectrum of ADDSA-1 in toluene, acetonitrile, DMSO, and methanol.

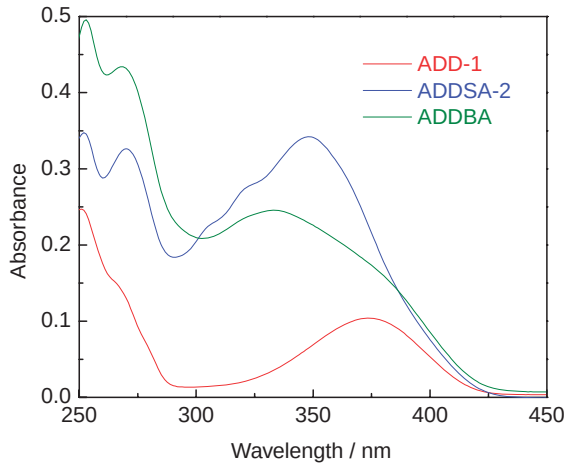

Fig. 3. Absorption spectrum of ADD-1, ADDSA-2, and ADDBA dyes (16 μM) in acetonitrile.

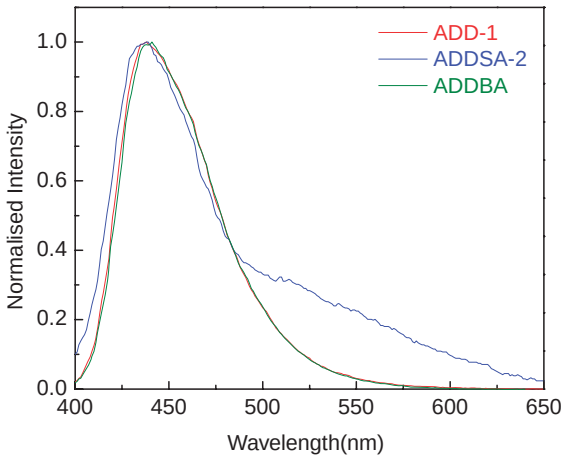

Fig. 4. Emission spectrum of ADD-1, ADDSA-2, and ADDBA dyes (16 μM) in acetonitrile.

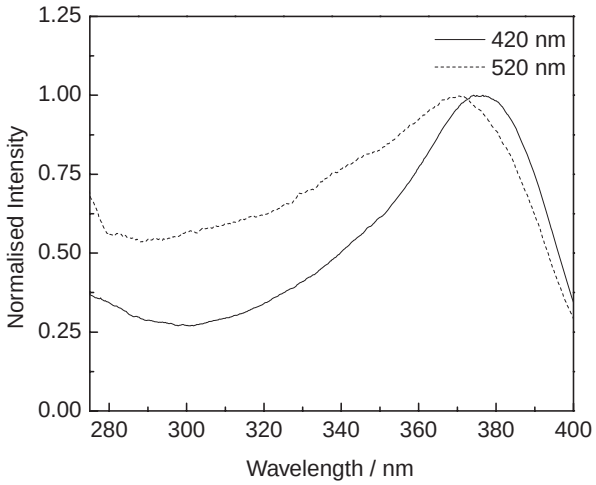

Fig. 5. Fluorescence excitation spectrum of ADDSA-1 in acetonitrile monitored at two different emission wavelengths.

It is known that the deprotonated form of the ADD dyes emits in the region of 500 to 520 nm.[32] To account for the anomalous emission at 528 nm, ADDSA-2 was prepared by substituting the methyl group in the place of ADD ring amino hydrogen. Table 1 lists the absorption and emission spectral characteristics of ADDSA-2 in various solvents. The absorption and emission spectrum of ADDSA-2 in acetonitrile is shown in Figs. 3 and 4, respectively. The presence of the anomalous longer wavelength emission peak for ADDSA-2 in aprotic solvents rules out the possibility of anomalous emission due to ADD ring amino hydrogen deprotonation. The presence of methyl group at the 10th position stabilizes the CT within the ADD moiety, which results in the unresolved LE and anomalous emission in aprotic solvents.

Is Photoinduced Electron Transfer (PET) Responsible for the Anomalous Longer Wavelength Emission? In our earlier photophysical studies on the bichromophoric donor–acceptor coupled 9-(4-dimethylamino-phenyl)-3,3,6,6-tetramethyl-3,4,6,7,9,10-hexahydro-2*H*,5*H*-acridine-1,8-dione (DMAADD) system, PET from the donor moiety (*N*,*N*-diethylaniline) to the ADD acceptor causes an emissive CT state that is responsible for the longer wavelength anomalous emission.[26] The CT state has larger dipole moments than that of the S_0 and LE states; therefore, the relative energy of the CT state against that of the LE state depends upon the solvent polarity. In ADDSA systems, the anomalous longer wavelength emission maximum is independent of solvent polarity. This clearly rules out the possibility that the longer wavelength emission is due to the CT state formed via PET between SA and ADD moieties.

Is Dual Fluorescence Originating from Two Different Chromophores? The fluorescence excitation spectra of ADDSA-1 in acetonitrile monitored at two different emission maximum (420 and 520 nm) are shown in Fig. 5. Two distinct excitation bands were observed, one at 370 nm and the other at 363 nm, corresponding to LE state and anomalous emission, respectively. The excitation spectrum recorded at the longer wavelength emission maximum also shows a broad shoulder around 340 nm, which was not seen in the excitation spectrum recorded at the shorter wavelength emission maximum. The above result indicates that the dual emission bands originate from two different chromophores of the same molecule. In order to confirm the above result, the 3D emission spectral

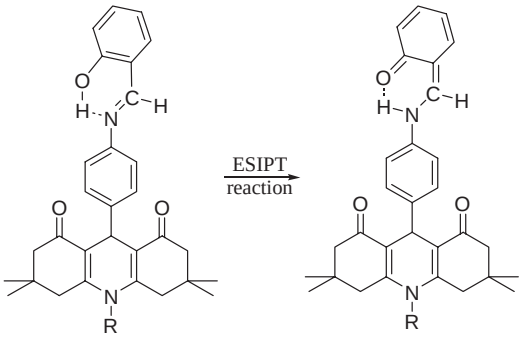

Scheme 2.

studies were performed. The 3D spectrum recorded for ADDSA-1 in acetonitrile is shown in Fig. S1. In acetonitrile, two contours were observed, and the corresponding excitation spectrum showed two bands at 370 and 363 nm. The excitation band observed at 370 nm corresponds to LE emission from ADD. The excitation band observed at 363 nm corresponds to anomalous emission. The excitation and 3D spectra confirm that the dual fluorescence in ADDSA-1 originates from two different chromophores. Due to the above reason, the excitation spectrum recorded at two different emission maxima was different from the absorption spectrum.

Is Anomalous Emission Due to an ESIPT Reaction with in the SA Moiety? The non-conjugated, but covalently linked, bichromophoric ADDSA systems consist of ADD and SA chromophores. ADD dyes show absorption maximum around 360 nm due to the CT from the ring nitrogen to ring carbonyl oxygen center.[31] SA compounds are characterized by a broad intense band at 340 nm.[33] The 350 nm absorption band of ADDSA-1 system is the overlap of two electronic transitions, that is, one CT absorption within ADD moiety (around 360 nm) and one electronic transition involving the SA moiety (around 340 nm) (Scheme 2).

Overlap of both the electronic transitions result in the absorption maximum of ADDSA systems around 350 nm. Figure 6 shows the emission spectra of ADDSA-1 in acetonitrile at different excitation wavelengths. The overlapping of electronic absorption of two chromophores caused the dual fluorescence at all the wavelengths of excitation in the region from 300 to 400 nm. At the blue edge of excitation anomalous fluorescence was dominant, while at the red edge of excitation, LE state emission was dominant.

The fluorescence spectra of SA compounds are characterized by a weak emission band around 530 nm region. The origin of this emission band has been previously attributed to excited keto tautomer species generated by a very fast enol-imine* to *cis*-keto amine* ESIPT.[1,34] From the above results, the longer wavelength anomalous emission of ADDSA systems at 530 nm was attributed to the excited state intramolecular proton-transfer reaction in the excited state of SA chromophore. Fluorescence quantum yield of ADDSA systems were extremely low ($\approx 10^{-4}$), which indicates that ESIPT acts as a main nonradiative channel for deactivation in the excited state. Perhaps the strongest support for this ESIPT is given by the non-proton transfer model system ADDBA. The absorption

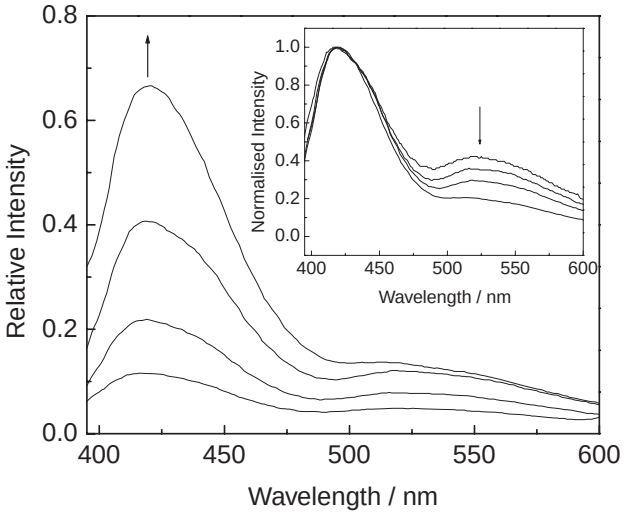

Fig. 6. Emission spectrum of ADDSA-1 in acetonitrile at various excitation wavelengths. λ_{exc} is (from top to bottom) 310, 330, 350, and 380 nm. Inset the normalised emission spectra for the same set [λ_{exc} is (from top to bottom) 310, 330, 350, and 380 nm].

and emission spectrum of ADDBA in acetonitrile are shown in Figs. 3 and 4. The emission spectrum of ADDBA was similar to the emission spectrum of ADD dye without the SA moiety (ADD-1). The absorption and emission spectral characteristics of ADDBA are presented in Table 1. Unlike ADDSA systems, ADDBA exhibited a single fluorescence band around 440 nm in all protic and aprotic solvents studied. In ADDBA, the observed emission around 430 nm is only due to the intramolecular CT from the ring nitrogen to the ring carbonyl oxygen centre within the ADD moiety. The emission around 430 nm was found to shift towards lower energies with an increase in the solvent polarity, and this shift is due to the stabilization of CT state. In contrast to the emission, the absorption spectra are due to the overlap of electronic transitions from two different chromophores of the same molecule (both BA and ADD moieties). In protic solvents, the hydrogen-bonding interaction of solvent proton with the imine proton may destabilize the electronic transition of the BA moiety. In order to confirm that, a detailed study is needed for ADDBA system. Because in ADDBA itself, two different processes are operative (CT within the ADD moiety and electronic transition within the BA moiety).

Absorption and emission spectral studies for ADDSA-1 in acetonitrile and methanol mixture were carried out. There was no significant change in the absorption spectrum of ADDSA-1 upon increasing the percentage of methanol. In contrast to the absorption spectrum, the normalized fluorescence spectrum presented in Fig. S2 (Supporting Information) showed a decrease in the fluorescence intensity of longer wavelength band along with a red shift in the emission maximum of LE as the percentage of methanol was increased. This clearly indicates that there is intermolecular interaction between the SA moiety with the protic solvents weakening the ESIPT pathway.

Time-Resolved Fluorescence Studies. In the previous time-resolved studies of the SA compound, time-domain or frequency domain techniques with pico- or femtosecond reso-

lution have been used.[33–36] In our time-resolved study, we used time-domain technique with both picosecond and femtosecond resolution. Figure 7 presents the fluorescence decay profiles of ADDSA-1 in acetonitrile at both the emission maximum. The fluorescence decay parameters of ADD systems in acetonitrile are listed in Table 2. In aprotic solvents, both the ADDSA-1 and ADDSA-2 systems had a shorter lifetime component (≈34 ps) in the larger fraction. Another component having longer lifetime (2.57 ± 0.06 ns for ADDSA-1 and 7.80 ± 0.06 ns for ADDSA-2) with smaller contribution was also obtained. Due to the limitation of picosecond instrument response function (≈52 ps), femto-upconversion studies were carried out to find the exact lifetime of short-lived component. The lifetime for ADDSA-1 (Fig. S3) and ADDSA-2 was 13 ± 2 ps. Our shorter lifetime components are in good agreement with $\tau = 10 \pm 3$ ps in acetonitrile, found by Ziolek et al. for *N*,*N*′-bis(salicylidene)-*p*-phenylenediamine (BSP).[35] Recently, Vergas has reported the biexponential decay for the substituted SA compounds in cyclohexane and alcoholic solution. The shorter lifetime component is about 0.02 ns, and the longer lifetime component is about 1.5 ns. His model considers the *cis*-keto* tautomer associated with the shorter lifetime component in a larger fraction.[33] From the earlier literature, the shorter component observed for the ADDSA systems corresponds to the decay of proton-transferred keto form. CT within the ADD moiety is responsible for the decay of longer component with smaller fraction. From the upconversion results, it should be noted that no rise component was observed. When the decay time of the longer wavelength state is smaller than that of the shorter wavelength state and when the longer wavelength state is formed out of the shorter wavelength state, the pre-exponential factor of the longer wavelength state should be negative (rise time) at all wavelengths. Therefore, the absence of such a term in the time-resolved decay also supports the hypothesis that the two-state decay is independent in nature and that there is no mother–daughter relationship between the two states. The former conclusion was supported by the absence of short-lived component (13 ps) in the non-proton transfer model system ADDBA. ADDBA showed biexponential decay with a lifetime of 0.68 ± 0.02 ns (96%) and 1.73 ± 0.02 ns (4%). PET from the BA to ADD acceptor is responsible for the shorter component, and LE state decay (CT within ADD moiety) is responsible for the longer component. Similar biexponential decay has been observed in non-proton transfer bichromophoric DMAADD system (0.66 and 1.98 ns in acetonitrile).[26] In contrast to ADDSA and ADDBA systems, ADD-1 showed single-exponential fluorescence decay (7.54 ± 0.02 ns) in acetonitrile due to the absence of both ESIPT and PET pathways. The ϕ_f values of ADDBA and ADD-1 in acetonitrile were found to be ≈0.0092 (±5%) and 0.63 (±0.02), respectively. PET is quite efficient in ADDBA, and this is evident from its low fluorescent quantum yield in comparison with that of ADD-1 without the donor moiety.

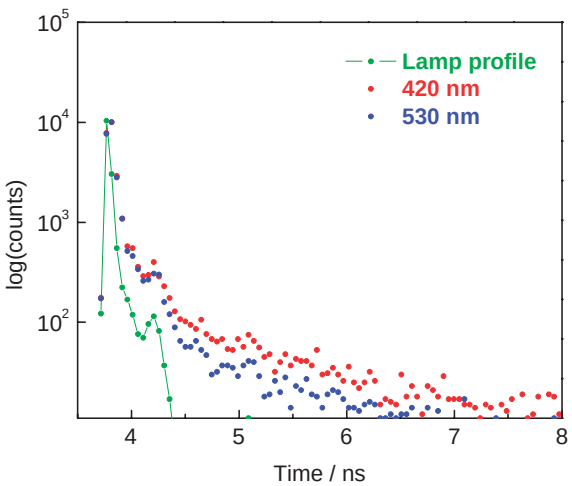

Fig. 7. Fluorescence decay profiles of ADDSA-1 monitored at 420 and 530 nm in acetonitrile. $\lambda_{exc} = 375$ nm.

Effect of Zn^{2+} on the Dual Fluorescence. In the first row transition metal ions, Zn^{2+} is photophysically inactive. It does not display any electron-transfer and energy-transfer processes due to completely filled d orbital. In order to confirm that the longer wavelength emission is due to an ESIPT reaction, photophysical studies were carried out in the presence of Zn^{2+} in acetonitrile for ADDSA systems. When Zn^{2+} was added to the ADDSA systems in acetonitrile, in the absorption spectrum, the absorbance at 350 nm decreased, and a new shoulder around 425 nm appeared. Figure 8 shows the effect of Zn^{2+} on the absorption spectra of ADDSA-1 in acetonitrile. The decrease in the absorbance at 350 nm in the presence of Zn^{2+} suggests that there is an interaction between metal ion and the SA moiety in the ground state. Unlike the absorption spectrum, the emission spectrum showed fluorescence enhancement in the presence of Zn^{2+} along with a red shift of 10 nm as depicted in Fig. 9. The water molecules present in the hydrated Zn^{2+} increase the solvent polarity around the ADDSA systems resulting in the stabilisation of CT state. We carried out blank experiments by taking the same amount of water molecules present in the hydrated form of $Zn(ClO_4)_2$, which gave less than one fold increase in the fluorescence intensity of the LE state ruling out the possibility of enhancement due

Table 2. Fluorescence Lifetime of ADDSA-1, ADDSA-2, ADDBA, and ADD-1 in Acetonitrile[a)]

	LE state[a)]		530 nm	
Dyes	τ_1/ns	τ_2/ns	τ_1/ns	τ_2/ns
ADDSA-1	≈0.034 (95)	2.57 ± 0.06 (5)	≈0.034 (98)	2.57 ± 0.06 (2)
ADDSA-2	≈0.034 (96)	7.80 ± 0.06 (4)	≈0.034 (97)	7.80 ± 0.06 (3)
ADDBA	0.68 ± 0.02 (96)	1.73 ± 0.02 (4)	0.68 ± 0.02	—
ADD-1	7.54 ± 0.02	—	7.54 ± 0.02	

a) Excitation wavelength 375 nm and fluorescence decay were monitored at 420 nm (ADDSA-1) and 440 nm (ADDSA-2, ADDBA, and ADD-1) for LE state. Amplitude (in parentheses).

to hydrated water molecules present in the Zn^{2+}. In ADDSA systems, ESIPT is the main nonradiative decay pathway probably due to the presence of SA moiety. Binding of Zn^{2+} with SA moiety suppresses the ESIPT pathway, resulting in the fluorescence enhancement with an increase in the concentration of metal ion.

The effect of Zn^{2+} on the fluorescence decay of ADDSA systems in acetonitrile was studied. Figure 10 presents the fluorescence decay profiles of ADDSA-1 at different concentration of Zn^{2+} in acetonitrile. The shorter component amplitude decreased gradually with an increase in the amplitude of longer component (2.57 ns for ADDSA-1 and 7.80 ns for ADDSA-2) upon increasing the concentration of Zn^{2+} in acetonitrile at both emission maximum. An increase in the lifetime of the longer component in the presence of Zn^{2+} and the disappearance of the short component is in accordance with the metal ion-induced suppression of ESIPT in the ADDSA systems (Scheme 3).

The steady state and time-resolved characteristics of ADDSA system suggests that the dual fluorescence originates from two different chromophores of the same molecule. The shorter wavelength emission around 430 nm is due to the CT within the ADD fluorophore. The solvent polarity independent longer wavelength anomalous emission originates from the keto form of the SA moiety via ESIPT in the excited state.

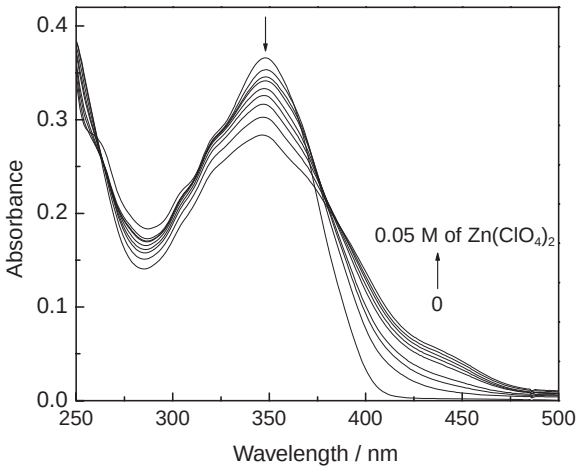

Fig. 8. Absorption spectrum of ADDSA-1 (16 μM) in the presence and absence of $Zn(ClO_4)_2$ in acetonitrile.

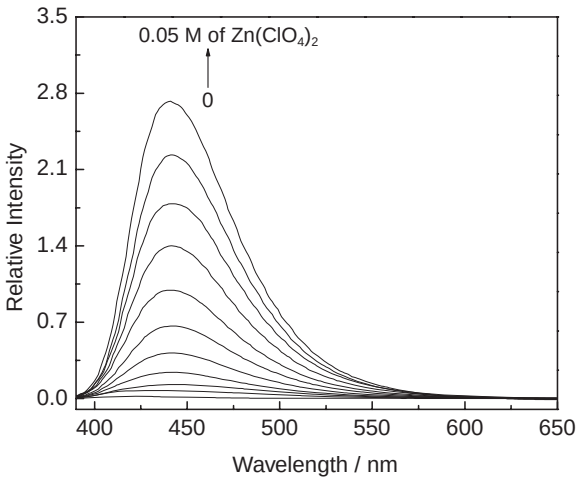

Fig. 9. Emission spectrum of ADDSA-1 (16 μM) in acetonitrile in the absence and presence of $Zn(ClO_4)_2$. $\lambda_{exc} = 378$ nm.

Conclusion

Nonconjugated, but covalently linked, bichromophoric systems ADDSA-1 and ADDSA-2 showed dual fluorescence in aprotic solvents. The shorter wavelength emission around 430 nm is due to the CT within the ADD fluorophore, which

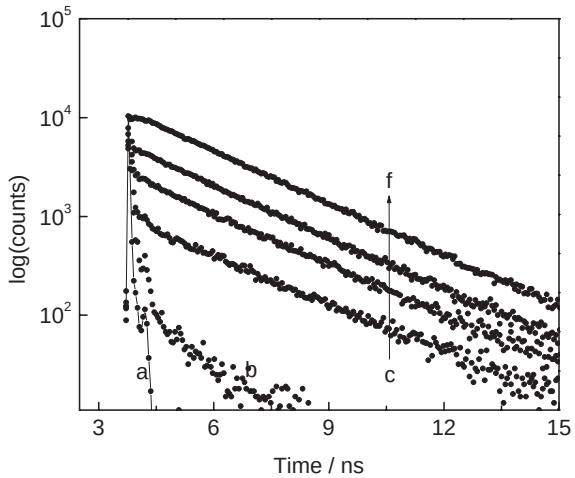

Fig. 10. Fluorescence decay profiles of ADDSA-1 (16 μM) in the absence (b) and presence of $Zn(ClO_4)_2$ in acetonitrile. $\lambda_{exc} = 375$ nm and $\lambda_{em} = 420$ nm. (a) is the laser profile; (c–f) 8 to 469 mM of $Zn(ClO_4)_2$.

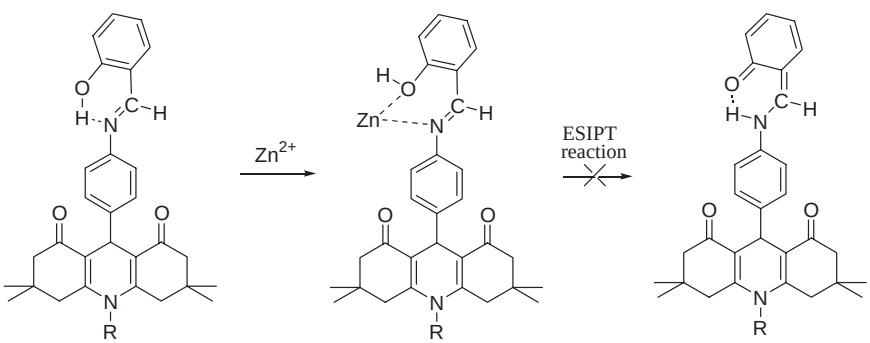

Scheme 3.

was found to shift towards lower energies with an increase in the solvent polarity and is due to the stabilisation of the CT state. In contrast to the lower wavelength emission, the anomalous longer wavelength emission maximum was independent of solvent polarity, and it was more pronounced in aprotic nonpolar solvents. Steady state and time-resolved measurement showed that the longer wavelength anomalous emission around 528 nm is due to the excited state intramolecular proton-transfer reaction in the SA chromophore. The fluorescence lifetime of the longer wavelength (530 nm) keto tautomer was found to be the same order as the shorter component in the shorter wavelength (420 nm). In presence of Zn^{2+}, the decrease in the relative amplitude of the shorter component confirms the metal ion-induced suppression of ESIPT in the ADDSA systems.

The above ESIPT state was confirmed by the ADDBA molecule (the absence of hydroxy group blocs the ESIPT pathway). In this molecule the absence of shorter component clearly reveals that in ADDSA series ESIPT mechanism plays a key role and results in the longer wavelength anomalous emission.

Experimental

General. Methanol, acetonitrile, dichloromethane, acetone, DMSO, and toluene used in this investigation were of HPLC grade purchased from Qualigens India Ltd. Zinc perchlorate used in the photophysical studies was purchased from Aldrich. Dimedone used for the preparation of ADD dyes was purchased from Ubichem (India) Ltd. Salicylaldehyde, benzaldehyde, methylamine, and *p*-nitrobenzaldehyde were purchased from E. Merck.

Synthesis of Acridinedione Dyes. ADD-1 was synthesized by the procedure reported in the literature.[37] The synthetic route for ADDSA and ADDBA are given in Scheme 4. AADD systems (AADD-1 and AADD-2) were synthesized according to the published work.[30]

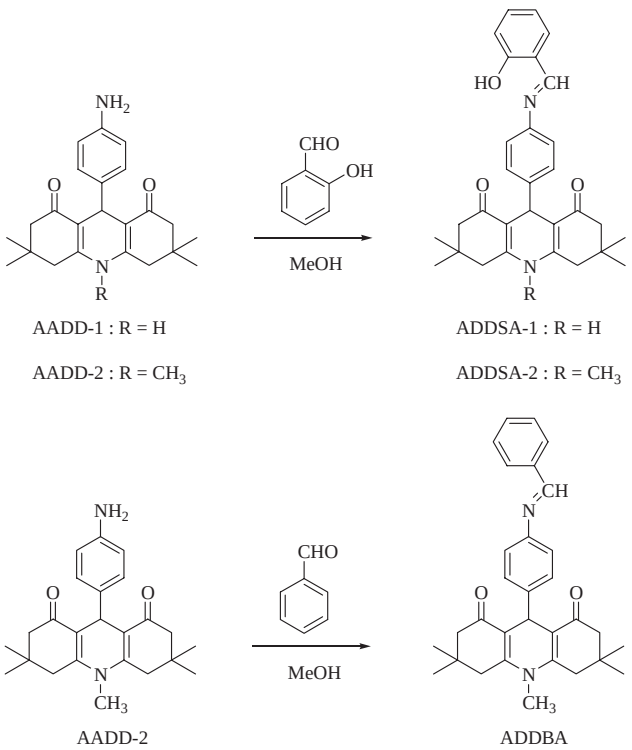

Scheme 4.

Synthesis of 9-(4-Salicylideneaminophenyl)-3,3,6,6-tetramethyl-3,4,6,7,9,10-hexahydro-1,8(2*H*,5*H*)-acridinedione (ADDSA-1): A mixture of the aminophenylacridinedione AADD-1 (1.0 g, 2.7 mmol) and salicylaldehyde (0.33 g, 2.7 mmol) in methanol (20 mL) was stirred at room temperature for 12 h. After completion, the reaction mixture was concentrated and cooled. The separated solid was collected by filtration and dried under vacuum. The product was purified by column chromatography over silica gel using 5% methanol in chloroform as eluent.

Yield: 1.10 g (86%); mp: 260–262 °C; IR (KBR): 3463, 3286, 3193, 2950, 1624, 1485 cm^{-1}; ^1H NMR (400 MHz, $CDCl_3$, TMS): δ 0.96 and 1.07 (2s, 12H, *gem*-dimethyl), 2.13–2.37 (m, 8H, C_2, C_4, C_5, C_7–CH_2), 5.12 (s, 1H, C_9–H), 6.89–7.47 (m, 8H, Ar–H), 7.77 (s, 1H, –N=CH), 8.52 (s, 1H, NH), 13.35 (s, 1H, –OH); ^{13}C NMR (100 MHz, $CDCl_3$, TMS) δ 27.14, 29.54, 32.64, 33.49, 40.83, 50.84, 113.11, 117.11, 119.04, 119.27, 120.81, 129.09, 132.20, 132.91, 145.73, 146.16, 148.97, 161.04, 161.87, 195.74; MS, *m*/*z* (%) 468 (M^+, 49); Analysis calculated for $C_{30}H_{32}N_2O_3$: C, 76.89; H, 6.88; N, 5.98%. Found: C, 76.98; H, 7.05; N, 6.17%.

Synthesis of 9-(4-Salicylideneaminophenyl)-3,3,6,6,10-pentamethyl-3,4,6,7,9,10-hexahydro-1,8(2*H*,5*H*)-acridinedione (ADDSA-2): By following the above procedure, reaction of the aminoacridinedione AADD-2 (1.0 g, 2.6 mmol) with salicylaldehyde (0.32 g, 2.6 mmol) afforded the Schiff base ADDSA-2.

Yield: 1.18 g (93%); mp: 280–282 °C; IR (KBR): 3436, 2950, 1635, 1473, 1369 cm^{-1}; ^1H NMR (400 MHz, $CDCl_3$, TMS): δ 1.04 and 1.09 (2s, 12H, *gem*-dimethyl), 2.21 (s, 4H, C_2 and C_7–CH_2), 2.36–2.65 (2d, 4H, J = 16.8 Hz, C_4 and C_5–CH_2), 3.30 (s, 3H, N–CH_3), 5.28 (s, 1H, C_9–H), 6.90–7.35 (m, 8H, Ar–H), 8.55 (s, 1H, –N=CH), 13.43 (s, 1H, –OH); ^{13}C NMR (100 MHz, $CDCl_3$, TMS): δ 28.69, 31.80, 32.71, 33.43, 40.68, 49.95, 114.95, 117.16, 118.94, 120.88, 128.70, 132.13, 132.80, 144.98, 151.01, 161.66, 195.31; MS, *m*/*z* (%) 482 (M^+, 37); Analysis calculated for $C_{31}H_{34}N_2O_3$: C, 77.15; H, 7.10; N, 5.80%. Found: C, 77.28; H, 7.33; N, 5.99%.

Synthesis of 9-(4-Benzylideneaminophenyl)-3,3,6,6,10-pentamethyl-3,4,6,7,9,10-hexahydro-1,8(2*H*,5*H*)-acridinedione (ADDBA): By following the above procedure, reaction of the aminoacridinedione AADD-2 (1.0 g, 2.6 mmol) with benzaldehyde (0.29 g, 2.6 mmol) afforded the Schiff base ADDBA.

Yield: 1.08 g (89%); mp: 232–235 °C; IR (KBR): 2956, 1629, 1572, 1105 cm^{-1}; ^1H NMR (400 MHz, $CDCl_3$, TMS): δ 1.02 and 1.07 (2s, 12H, *gem*-dimethyl), 2.23 (s, 4H, C_2 and C_7–CH_2), 2.34–2.63 (2d, 4H, J = 16.7 Hz, C_4 and C_5–CH_2), 3.28 (s, 3H, N–CH_3), 5.28 (s, 1H, C_9–H), 7.03–7.85 (m, 9H, Ar–H), 8.40 (s, 1H, –N=CH); ^{13}C NMR (100 MHz, $CDCl_3$, TMS): δ 28.69, 31.47, 32.65, 33.39, 40.59, 49.92, 114.95, 120.63, 128.32, 128.65, 131.02, 136.38, 143.84, 149.68, 150.98, 151.09, 159.53, 195.32; MS, *m*/*z* (%) 466 (M^+, 42); Analysis calculated for $C_{31}H_{34}N_2O_2$: C, 79.79; H, 7.34; N, 6.00%. Found: C, 79.92; H, 7.52; N, 6.13%.

Techniques. Absorption spectra were recorded on an Agilent 8453 diode array spectrophotometer. Fluorescence spectral measurements were carried out using a Perkin-Elmer MPF-44B fluorescence spectrophotometer interfaced to a PC through a RISHCOM-100 multimeter. IR spectra were recorded on a FTIR-8300 Shimadzu spectrophotometer. ^1H NMR and ^{13}C NMR spectra were recorded on Jeol-GSX 400 (400 MHz) instrument with TMS as internal standard (chemical shift in δ ppm). The mass spectra were recorded with a Jeol-JMS-DX 303 HF instrument.

Fluorescence decays were recorded using the TCSPC method using the following setup. A diode pumped millena CW laser

(Spectra Physics) at 532 nm was used to pump the Ti:sapphire rod in Tsunami picosecond mode locked laser system (Spectra Physics). The 750 nm (80 MHz) light was taken from the Ti:sapphire laser and passed through pulse picker (Spectra Physics, 3980 2S) to generate 4 MHz pulses. The second harmonic output (375 nm) was generated by a flexible harmonic generator (Spectra Physics, GWU 23PS). The vertically polarized 375 nm laser was used to excite sample. The fluorescence emission at a magic angle (54.7°) was dispersed in a monochromator (f/3 aperture), counted by an MCP PMT (Hamamatsu R 3809) and processed through CFD, TAC, and MCA. The instrument response function for this system was ≈52 ps. The fluorescence decay was analysed by using the software provided by IBH (DAS-6) and PTI global analysis software.

Shorter components of the fluorescence decay of the dyes were recorded using a femtosecond upconversion spectrometer. The sample solution was excited with frequency doubled laser pulse (395 nm) generated by coupling FOG-100 (CDP, Russia) with a 60 fs Ti-sapphire Laser (Tsunami, Spectra Physics). The polarization of the excitation beam for magic angle condition was controlled with a Berek compensator. The rotating sample cuvette was 1 mm thick. The horizontally polarized fluorescence emitted from the sample was upconverted in a BBO crystal with residual IR gate pulse passing through a variable delay line with a resolution of 6.25 fs. Spectral resolution was achieved by dispersing the upconverted light in a spectrometer with single monochromator and a photon counter. The FOG-100 had a 350 fs (FWHM) cross correlation function and maximum time delay of 1.7 ns. The fluorescence decay curves were fitted with windows based LUMEX 3.1 software (CDP), and the quality of fit was judged from the χ^2.

Fluorescence quantum yield was obtained from the corrected fluorescence spectrum using the expression;

$$\phi_f = (A_s/A_r)(a_r/a_s)(n_s/n_r)^2 \times 0.546, \quad (1)$$

where, A_s and A_r are the area under the corrected fluorescence spectrum, a_s and a_r are the absorbances at the wavelength of excitation (366 nm), n_s and n_r are the refractive indices of the solvent for the sample and reference, respectively. The absorbance value was adjusted to 0.02. The area under the spectra was obtained by numerically integrating the area using Simpson's method. Quinine sulfate in 0.05 mol L^{-1} sulfuric acid was used as the reference for quantum yield determination (ϕ_f of quinine sulfate = 0.546).

The authors acknowledge Council of Scientific and Industrial Research (CSIR) and Department of Science and Technology (DST), India for financial support. We also thank Dr. A. K. Mishra, IIT, Chennai for allowing access to the contour measurement facilities.

Supporting Information

3D contour plot of ADDSA-1 in acetonitrile; Femto-upconversion fluorescence decay of ADDSA-1; Fluorescence decay profiles of ADDSA-2 in acetonitrile; Absorption and emission spectrum of ADDSA-2 in the presence and absence of $Zn(ClO_4)_2$ in acetonitrile; Fluorescence decay profiles of ADDSA-2 in the presence of $Zn(ClO_4)_2$ in acetonitrile. This material is available free of charge on the web at http://www.csj.jp/journals/bcsj.

References

1 a) T. Elsaesser, H. J. Bakker, Ultrafast Hydrogen Bonding Dynamics and Proton Transfer Processes in the Condensed Phase, Kluwer, Dordrecht, **2002**. b) A. Weller, *Prog. React. Kinet.* **1961**, *1*, 188. c) S. M. Ormson, R. G. Brown, *Prog. React. Kinet.* **1994**, *19*, 45. d) D. LeGourrierec, S. M. Ormson, R. G. Brown, *Prog. React. Kinet.* **1994**, *19*, 211. e) S. J. Formosinho, L. G. Arnaut, *J. Photochem. Photobiol., A* **1993**, *75*, 21.

2 F. Vollmer, W. Rettig, E. Birckner, *J. Fluoresc.* **1994**, *4*, 65.

3 A. B. Kotlyar, N. Borovok, S. Kiryati, E. Nachliel, M. Gutman, *Biochemistry* **1994**, *33*, 873.

4 M. L. Martinez, W. C. Cooper, P.-T. Chou, *Chem. Phys. Lett.* **1992**, *193*, 151.

5 M. E. Kletskii, A. A. Millov, A. V. Metelitsa, M. I. Knyazhansky, *J. Photochem. Photobiol., A* **1997**, *110*, 267.

6 G. J. Stueber, M. Kieninger, H. Schettler, W. Busch, B. Goeller, J. Franke, H. E. A. Kramer, H. Hoier, S. Henkel, P. Fischer, H. Port, T. Hirsch, G. Rytz, J.-L. Birbaum, *J. Phys. Chem.* **1995**, *99*, 10097.

7 F. Vollmer, W. Rettig, *J. Photochem. Photobiol., A* **1996**, *95*, 143.

8 J. Catalan, *J. Am. Chem. Soc.* **2001**, *123*, 11940.

9 a) W. Rettig, R. Fritz, J. Springer, in *Photochemical Processes in Organized Molecular Systems*, ed. by K. Honda, Elsevier Science Publishers, Amsterdam, **1991**, p. 61. b) N. P. Ernsting, A. Mordzinski, B. Dick, *J. Phys. Chem.* **1987**, *91*, 1404. c) B. Dick, N. P. Ernsting, *J. Phys. Chem.* **1987**, *91*, 4261.

10 a) A. U. Acuna, F. Amat-Guerri, J. Catalan, F. Gonzalez-Tablas, *J. Phys. Chem.* **1980**, *84*, 629. b) F. Toribio, J. Catalan, F. Amat, A. U. Acuna, *J. Phys. Chem.* **1983**, *87*, 817. c) D. Gormin, M. Kasha, *Chem. Phys. Lett.* **1988**, *153*, 574. d) D. Gormin, *J. Phys. Chem.* **1989**, *93*, 5979. e) F. Lahmani, A. Zehnacker-Rentien, *J. Phys. Chem. A* **1997**, *101*, 6141.

11 a) J. Catalan, F. Toribio, A. U. Acuna, *J. Phys. Chem.* **1982**, *86*, 303. b) S. Mitra, R. Das, S. Mukherjee, *Chem. Phys. Lett.* **1993**, *202*, 549. c) P.-T. Chou, M. Chao, J. H. Clements, M. L. Martinez, C.-P. Chang, *Chem. Phys. Lett.* **1994**, *220*, 229.

12 a) S. Lochbrunner, K. Stock, E. Riedle, *J. Mol. Struct.* **2004**, *700*, 13. b) A. Mordziński, A. Grabowska, W. Kühnle, A. Kröwczyński, *Chem. Phys. Lett.* **1983**, *101*, 291. c) J. M. Kaufmann, P. T. Litac, W. J. Boyko, *J. Heterocycl. Chem.* **1995**, *32*, 1541.

13 a) M. Rini, A. Kummrow, J. Dreyer, E. T. J. Nibbering, T. Elsaesser, *Faraday Discuss.* **2003**, *122*, 27. b) M. Rini, J. Dreyer, E. T. J. Nibbering, T. Elsaesser, *Chem. Phys. Lett.* **2003**, *374*, 13. c) S. Lochbrunner, A. J. Wurzer, E. Riedle, *J. Phys. Chem. A* **2003**, *107*, 10580. d) R. de Vivie-Riedle, V. De Waele, L. Kurtz, E. Riedle, *J. Phys. Chem. A* **2003**, *107*, 10591. e) A. Heller, D. L. Williams, *J. Phys. Chem.* **1970**, *74*, 4473.

14 a) G. Woessner, G. Goeller, J. Rieker, H. Hoier, J. J. Stezowski, E. Daltrozzo, M. Neureiter, H. E. A. Kramer, *J. Phys. Chem.* **1985**, *89*, 3629. b) J. Rieker, E. Lemmert-Schmitt, G. Goeller, M. Roessler, G. J. Stueber, H. Schettler, H. E. A. Kramer, J. J. Stezowski, H. Hoier, S. Henkel, A. Schmidt, H. Port, M. Wiechmann, J. Rody, G. Rytz, M. Slongo, J.-L. Birbaum, *J. Phys. Chem.* **1992**, *96*, 10225.

15 a) A. J. G. Strandjord, D. E. Smith, P. F. Barbara, *J. Phys. Chem.* **1985**, *89*, 2362. b) M. Itoh, Y. Fujiwara, M. Sumitani, K. Yoshihara, *J. Phys. Chem.* **1986**, *90*, 5672. c) S. M. Ormson, R. G. Brown, F. Vollmer, W. Rettig, *J. Photochem. Photobiol., A* **1994**, *81*, 65.

16 a) S. J. Schmidtke, D. F. Underwood, D. A. Blank, *J. Am. Chem. Soc.* **2004**, *126*, 8620. b) F. V. R. Neuwahl, L. Bussotti, R. Righini, G. Buntinx, *Phys. Chem. Chem. Phys.* **2001**, *3*, 1277. c) T. P. Smith, K. A. Zaklika, K. Thakur, P. F. Barbara,

J. Am. Chem. Soc. **1991**, *113*, 4035. d) T. P. Smith, K. A. Zaklika, K. Thakur, G. C. Walker, K. Tominaga, P. F. Barbara, *J. Phys. Chem.* **1991**, *95*, 10465. e) T. P. Smith, K. A. Zaklika, K. Thakur, G. C. Walker, K. Tominaga, P. F. Barbara, *J. Photochem. Photobiol., A* **1992**, *65*, 165.

17 a) H. Bulska, A. Grabowska, Z. R. Grabowski, *J. Lumin.* **1986**, *35*, 189. b) P. Borowicz, A. Grabowska, A. Le, L. Kaczmarek, B. Zagrodzki, *Chem. Phys. Lett.* **1998**, *291*, 351.

18 M. Čuma, C. Thompson, S. Scheiner, *J. Comput. Chem.* **1998**, *19*, 129.

19 a) P.-T. Chou, W.-S. Yu, Y.-M. Cheng, S.-C. Pu, Y.-C. Yu, Y.-C. Lin, C.-H. Huang, C.-T. Chen, *J. Phys. Chem. A* **2004**, *108*, 6487. b) P.-T. Chou, C.-H. Huang, S.-C. Pu, Y.-H. Liu, Y. Wang, C.-T. Chen, *J. Phys. Chem. A* **2004**, *108*, 6452.

20 T. Sekikawa, T. Kobayashi, T. Inabe, *J. Phys. Chem. A* **1997**, *101*, 644.

21 a) M. D. Cohen, G. M. J. Schmidt, *J. Phys. Chem.* **1962**, *66*, 2442. b) K. Kownacki, A. Mordzinski, R. Wilbrandt, A. Grabowska, *Chem. Phys. Lett.* **1994**, *227*, 270.

22 a) A. Grabowska, K. Kownacki, J. Karpiuk, S. Dobrin, L. Kaczmarek, *Chem. Phys. Lett.* **1997**, *267*, 132. b) K. Kownacki, A. Mordzinski, R. Wilbrandt, A. Grabowska, *Chem. Phys. Lett.* **1994**, *227*, 270.

23 a) A. Ohshima, A. Momotake, T. Arai, *Chem. Lett.* **2005**, *34*, 1288. b) A. Ohshima, A. Momotake, T. Arai, *Bull. Chem. Soc. Jpn.* **2006**, *79*, 305.

24 K. J. Prabahar, V. T. Ramakrishnan, D. Sastikumar, S. Selladurai, V. Masilamani, *Indian J. Pure Appl. Phys.* **1991**, *29*, 382.

25 a) C. Selvaraju, P. Ramamurthy, *Chem. Eur. J.* **2004**, *10*, 2253. b) S. Singh, S. Chhina, V. K. Sharma, S. S. Sachdev, *J. Chem. Soc., Chem. Commun.* **1982**, 453.

26 a) V. Thiagarajan, C. Selvaraju, E. J. Padma Malar, P. Ramamurthy, *ChemPhysChem* **2004**, *5*, 1200. b) V. Thiagarajan, P. Ramamurthy, *ISRAPS Bull.* **2005**, *17*, 18.

27 a) V. Thiagarajan, V. K. Indirapriyadarshini, P. Ramamurthy, *J. Inclusion Phenom. Macrocyclic Chem.* **2006**, DOI: 10.1007/s10847-005-9043-4. b) R. Kumaran, P. Ramamurthy, *J. Phys. Chem. B* **2006**, *110*, 23783.

28 H. J. Timpe, S. Ulrich, C. Decker, J. P. Fouassier, *Macromolecules* **1993**, *26*, 4560.

29 H. J. Timpe, S. Ulrich, J. P. Fouassier, *J. Photochem. Photobiol., A* **1993**, *73*, 139.

30 a) V. Thiagarajan, P. Ramamurthy, D. Thirumalai, V. T. Ramakrishnan, *Org. Lett.* **2005**, *7*, 657. b) V. Thiagarajan, P. Ramamurthy, *Spectrochim. Acta, Part A* **2006**, doi:10.1016/j.saa.2006.08.031.

31 a) N. Srividya, P. Ramamurthy, V. T. Ramakrishnan, *Spectrochim. Acta, Part A* **1997**, *53*, 1743. b) N. Srividya, P. Ramamurthy, V. T. Ramakrishnan, *Spectrochim. Acta, Part A* **1998**, *54*, 245.

32 B. Venkatachalapathy, P. Ramamurthy, V. T. Ramakrishnan, *J. Photochem. Photobiol., A* **1997**, *111*, 163.

33 V. Vargas C., *J. Phys. Chem. A* **2004**, *108*, 281.

34 a) P. F. Barbara, P. M. Rentzepis, L. E. Brus, *J. Am. Chem. Soc.* **1980**, *102*, 2786. b) T. Sekikawa, T. Kobayashi, T. Inabe, *J. Phys. Chem. A* **1997**, *101*, 644.

35 M. Ziółek, J. Kubicki, A. Maciejewski, R. Naskrçcki, A. Grabowska, *J. Chem. Phys.* **2006**, *124*, 124518.

36 a) S. Mitra, N. Tamai, *Chem. Phys. Lett.* **1998**, *282*, 391. b) S. Mitra, N. Tamai, *Chem. Phys.* **1999**, *246*, 463.

37 N. Srividya, P. Ramamurthy, P. Shanmugasundram, V. T. Ramakrishnan, *J. Org. Chem.* **1996**, *61*, 5083.